DOI: 10.1021/ma1020193

Macromolecules
ARTICLE

Flow Memory and Stability of Shear-Induced Nucleation Precursors in Isotactic Polypropylene

Dario Cavallo,[†] Fiorenza Azzurri,[†] Luigi Balzano,[‡] Sérgio S. Funari,[§] and Giovanni C. Alfonso*,[†]

[†]*Dipartimento di Chimica e Chimica Industriale, Università di Genova, via Dodecaneso 31, 16146 Genova, Italy,* [‡]*Department of Mechanical Engineering, Eindhoven University of Technology P.O. Box 513, 5600 MB Eindhoven, The Netherlands, and* [§]*Hamburger Synchrotronstrahlungslabor (HASYLAB)/Deutsches Elektronen-Synchrotron (DESY), Notkestrasse 85, D-22603 Hamburg, Germany*

Received August 31, 2010; Revised Manuscript Received October 8, 2010

ABSTRACT: The dissolution of flow-induced nucleation precursors in isotactic polypropylene is investigated indirectly by means of in situ rheo-SAXS measurements. The progress of crystallization and the evolution of crystal orientation are recorded in isothermal conditions after a controlled shear step followed by an annealing step of different duration at various melt temperatures. The results confirm that the survival time of shear-induced nucleation precursors is extremely large compared to typical rheological relaxation times and it is longer for the precursors originated at higher shear rate. Most important, we show that the effect of flow on the development of oriented morphologies is lost much earlier than that on the overall crystallization kinetics. A schematic model for precursors' dissolution involving gradual transformation from row into point-like nuclei is proposed.

Introduction

Because of their intrinsic soft matter nature, the long and flexible chains constituting polymeric materials are easily oriented and stretched by flow fields in the molten state. The peculiarity of polymeric systems is that a "memory" of the resulting deformation can persist to the point that subsequent structure formation is substantially affected.[1] This is particularly evident in the processing of semicrystalline polymers, where the whole thermal and mechanical histories adopted to shape the product result in the development of oriented crystals as well as in an impressive enhancement of the crystallization kinetics. Despite flow induced crystallization of polymer melts has been extensively investigated during several decades because of its technological relevance,[2−6] a detailed and comprehensive description of underlying molecular mechanisms is still lacking. A large wealth of experimental evidence, gathered in the last years by coupling complementary techniques such as rheometry,[7−12] small angle X-ray scattering and wide angle X-ray diffraction (SAXS/WAXD),[13−16] birefringence and small angle light scattering (SALS),[17−22] and optical microscopy,[23−26] has led to a fair phenomenological description of the effects of flow on polymer crystallization.

The statement that shear flow promotes local alignment of chain segments and generates quasi-crystalline metastable nanodomains with an intermediate degree of order, usually referred to as crystal nucleation precursors, has attained a wide consensus.[13−18,21,26] It has been observed that these nucleation precursors, when generated by flow fields, can survive in quiescent conditions for very long time, even above the melting point of the crystals, and behave as active nuclei when the temperature is lowered, thus dramatically increasing the nucleation density and enhancing crystallization kinetics.[27] The formation and decay of flow-induced clusters of chain segments have been theoretically predicted[28] and even simulated by dynamic Monte Carlo methods.[29] However, because of the extremely small amount of mass involved in their formation, the small size and the low degree of order, the nature of these precursors is elusive and their experimental detection is actually challenging. This notwithstanding, several direct evidences of the existence of long-living metastable structures in sheared polymer melts have been reported.[30−38] On segmental scale, rheo-Raman spectra of sheared polyethylene melts indicate the presence of chain sequences in trans conformation, featuring the ordered crystalline state, which persist for several hours after cessation of the shear.[30] Recently, shear-induced conformational ordering in the molten state was also observed in samples of isotactic polypropylene by Li et al.[31−33] In this case, flow enhances the concentration of long sequences of repeating units in the 3/1 helical conformation required to form the monoclinic crystalline structure. A decay of the concentration of these helices, showing very long and strongly temperature-dependent characteristic time, was also reported.[32] Mesoscopic structures, consisting in a scaffold of row-nuclei onto which lamellae may develop, were also observed by means of rheo-SAXS in sheared i-PP melts.[15,34,35] These bundles of aligned chain segments can be generated by flow and linger for hours at temperatures as high as 185 °C, well above the actual melting point of the crystals.[35] The formation of a metastable suspension of shishes by imposing the shear close to the thermodynamic melting temperature was also reported by Balzano et al. for a bimodal HDPE.[36] The presence of threadlike precursors was proved with rheo-optical techniques by Kornfield et al.[17,37] in i-PP melt submitted to duct flow. They observed a peculiar upturn in the birefringence during flow up to a temperature of 215 °C; nevertheless, for temperatures higher than 205 °C, the flow induced structures relax so fast that no oriented structures were found in the recovered samples.[37]On larger dimensional scale, formation of micrometer-sized row-nucleated structures, visible by optical microscopy and detectable by light scattering, was reported by Kanaya et al. in isotactic polystyrene sheared above the nominal melting temperature.[38,39]

Together with the above-mentioned direct methods, formation and relaxation of shear induced precursors was also inferred from the investigation of flow memory effects on crystallization

*Corresponding author.

 Published on Web 10/26/2010

kinetics and morphology. In this context, the pioneering work of Janeschitz-Kriegl et al.[40−42] must be acknowledged. With clever duct flow experiments, they proved a gradual decay of the concentration of the shear-induced threadlike precursors formed in the skin layer by measuring the birefringence after a relaxation step at high temperature. The initial experiments with i-PP were later extended to i-PBu-1;[43] In both cases, it was shown that the underlying relaxation phenomena take place in a time scale which is much longer than the rheological one and exhibit a much stronger temperature dependence.[44] These results were confirmed, also on a quantitative basis, by the analogous experiments performed by Isayev et al.[45] Other researchers focused on the spherulitic morphology developing after a step shear, imposed either by fiber pulling[46] or with a plate−plate rotational device,[47] followed by annealing at the shearing temperature. The disappearance of precursors was suggested by the gradual increase of the average spherulitic radius with the annealing time. The thermal stability of shear-induced shish-kebab precursors was investigated by Zuo et al. by rheo-SAXS experiments on a model polyethylene blend.[48] The adopted thermal protocol, consisting in a succession of recrystallization steps after partial melting performed at increasing temperatures, enabled them to demonstrate the flow-induced precursors can withstand temperatures as high as 154 °C, remarkably higher than the thermodynamic melting point. Our group has been involved in the above issues since a long time.[49−51] By performing fiber-pulling experiments, and using the cylindritic morphology as a marker for the presence of high linear nucleation density, it was possible to determine the lifetime of shear-induced nucleation precursors in various semicrystalline polymers at several temperatures.[49,50] The results were in good agreement with those previously reported by Janeschitz-Kriegl et al.[40−42] Further experiments, performed on i-PBu-1 and i-PS, have shown that the characteristic relaxation time is strongly dependent on the weight-average molar mass of the polymer, both for polydispersed grades and narrow fractions.[50,52] A mechanism for precursor's dissolution, based on the detachment of chain stems from the lateral surface of cylindrical clusters, was proposed to explain the gathered experimental evidence.[52]

Notwithstanding the considerable experimental efforts in this field, some open questions still remain. For instance, it is not known if, and to what extent, the thermo-mechanical history in which the precursors are formed affects their morphological and structural features (length, diameter, degree of order). Therefore, the stability to thermal treatment of precursors generated in different conditions cannot yet be foreseen. In this paper we address the above issue by assessing the effect of precursor's relaxation on isothermal crystallization kinetics and crystal orientation.

Experimental Section

Materials and Techniques. The polymer used in this investigation is a commercial Ziegler−Natta isotactic polypropylene homopolymer (T30G Montell, Ferrara) with weight-average molar mass of 376 kg/mol, polydispersity index (M_w/M_n) of 6.7, MFI of 3.6 dg/min and a meso pentads content of 87.6%.[53]

Films around 400 μm thick were first obtained from the supplied pellets by compression molding at 210 °C for 5 min and subsequent quenching in air. Disks of approximately 14 mm diameter were cut from the molded films for the rheo-SAXS experiments.

Time-resolved SAXS measurements during crystallization were carried out at the A2 soft-condensed matter beamline of HASYLAB-DESY (Hamburg) using a synchrotron X-ray beam with wavelength $\lambda = 1.5$ Å. The SAXS patterns were collected by a 2D MARCCD detector with a resolution of 1024 × 1024 pixels. The sample to detector distance, calibrated by acquiring the pattern of an oriented sample of dry rat-tail collagen (spacing = 65 nm), was 2563 mm. An exposure time of 25 s was used, with a waiting time of 5 s between subsequent frames. All X-ray data were corrected for background (air and instrument) scattering before analysis.

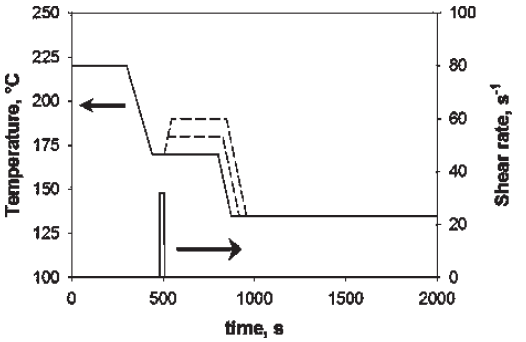

Figure 1. Scheme of the adopted thermo-mechanical protocol.

Temperature and deformation history was imposed by a Linkam CSS450 shearing cell, which has widely been used for in situ rheo-X-ray experiments.[13−16] To allow the transmission of X-rays, the original quartz plates of the shear cell are usually replaced by metal disks in which holes are drilled and covered by a thin Kapton film. Preliminary tests of this configuration revealed us that replacement of a low thermal conductivity material with a metal remarkably affects temperature uniformity along the radius and leads to relevant discrepancies between the actual sample temperature and the set value. To overcome this problem, the windows were drilled directly in the original quartz plates. A single hole, around 4 mm diameter, was made in the stationary plate and three holes, at 120°, were drilled in the rotating one. A Kapton film, 100 μm thick, was then fixed on the plates by means of a high temperature glue. Coincidence between the temperature in sample and the one imposed by the controller was proved by means of a microthermocouple embedded in the polymer film. It has been ascertained that, in the adopted heating and cooling conditions, a sample thickness of 200 μm rules out any meaningful thermal lag.

In Situ Rheo-SAXS Experiments. The applied thermo-mechanical history is schematically shown in Figure 1. The sample was first heated to 220 °C, well above the equilibrium melting temperature of the crystals, and the gap between the plates of the shearing cell was slowly reduced to 200 μm. The polymer was then held at this temperature for 5 min, to erase any memory of previous treatments, and subsequently cooled to the shearing temperature, T_s, at the highest possible cooling rate of 30 °C/min. In order to prevent crystallization at this stage, the shear step was imposed at 170 °C, above the actual melting point of polypropylene spherulites. To investigate the effect of flow conditions on precursors' stability, a shear pulse of constant duration of 5 s was imposed at two different shear rates of 16 and 32 s^{-1}. The shear-induced precursors were then left to partially relax in the subsequent step. Relaxation of flow memory has been carried out in a temperature range between T_s and 190 °C for a time period spanning from 0 to 45 min. When the relaxation was carried out at temperatures higher than T_s, the sample was heated at the maximum rate of 30 °C/min. The system was finally brought to 135 °C, where the extent of the relaxation process was assessed by following the isothermal crystallization kinetics through time-resolved SAXS.

SAXS Data Analysis. SAXS patterns were analyzed using the Fit-2D software.[54] At first, 2-D SAXS images were azimuthally averaged and radially integrated to extract the 1-D intensity profiles, I(q), as a function of the scattering vector $q = 4\pi(\sin\theta)/\lambda$, where 2θ is the scattering angle. From these data the relative invariant, Q_S, defined as

$$Q_s = \int_0^\infty q^2 I(q)\,\mathrm{d}q \approx \int_{q_2}^{q_2} q^2 I(q)\,\mathrm{d}q \qquad (1)$$

was calculated. The adopted integration limits q_1 and q_2 were 0.15 and 0.45 nm^{-1}, respectively. The time evolution of the relative invariant enabled us to follow the kinetics of quiescent

isothermal primary crystallization[55] after the applied thermomechanical history.

The degree of orientation of the developing lamellar structures was estimated from the value of the Hermans orientation factor,[56,57]

$$f_H = \frac{3(\cos^2 \phi)}{2} - 1 \tag{2}$$

where $\langle \cos^2 \varphi \rangle$ is the average cosine squared of the angle between the perpendicular to the scatterers (lamellar stacks) and the flow direction, and is given by

$$\langle \cos^2 \varphi \rangle = \frac{\int_0^{\pi/2} I(\beta) \cos^2(\beta) \sin(\beta)\, d\beta}{\int_0^{\pi/2} I(\beta) \sin(\beta)\, d\beta} \tag{3}$$

with β representing the azimuthal angle in the diffraction pattern.

To calculate the Hermans orientation factor, the angular variation of the intensity was extracted from the 2-D SAXS data through an azimuthal scan ($I(\beta)$), obtained by averaging the intensity over a small q region centered around the value of the peak in the radial intensity profile (about 0.3 nm^{-1}).

According to literature suggestions,[16,58] a sector-averaged integration of the 2-D SAXS patterns was performed to investigate the effects of flow and subsequent relaxation on anisotropic development of the morphology. Two azimuthal sectors of identical angular width (45°), centered along the flow direction and perpendicular to it, were considered. The radial intensity profiles $I(q)$, obtained from the above procedure were then integrated in the same q-range adopted for the relative invariant.

Results and Discussion

Effect of Flow and Relaxation on the Crystallization Kinetics. Representative examples of crystallization curves obtained by normalizing the relative invariants between 0 and 1 are shown in Figure 2a. They refer to quiescent, sheared and partially relaxed samples.

It is evident that the crystallization kinetics is the fastest when the specimen is cooled to the crystallization temperature, T_c, immediately after the cessation of flow. Much slower progress of crystallization is observed when the polymer is held to relax for some time at high temperature and even slower when no shear is imposed, i.e., under quiescent conditions. Consistently with the concept that the flow induced metastable precursors progressively dissolve if they are held at temperatures above the polymer melting point,[49−51] the flow-induced enhancement of crystallization kinetics slowly fades away and its complete disappearance is expected if a sufficiently long holding time in the melt is interposed between the shear impulse and the cooling to T_c. The increase of nucleation density originated by flow is also reflected by its dramatic effect on the induction time. Development of crystallinity in the sheared polymer begins as soon as the crystallization temperature is reached; on the contrary, at the same temperature, a certain time is needed to detect the onset of crystallization in quiescent conditions.

In principle, one can think to use Avrami equation to extract quantitative information on the actual concentration of active nuclei from the curves shown in Figure 2a. In facts, for the used polypropylene, the values of the linear crystal growth rates are available in a wide temperature range[59] and it is also known that the growth rate in quiescent conditions is independent of previous shear history.[26] Unfortunately, the hypotheses on which Avrami equation was derived do not hold when development of oriented or mixed morphologies occurs; non avramian crystallization mechanism and anomalous values of the Avrami

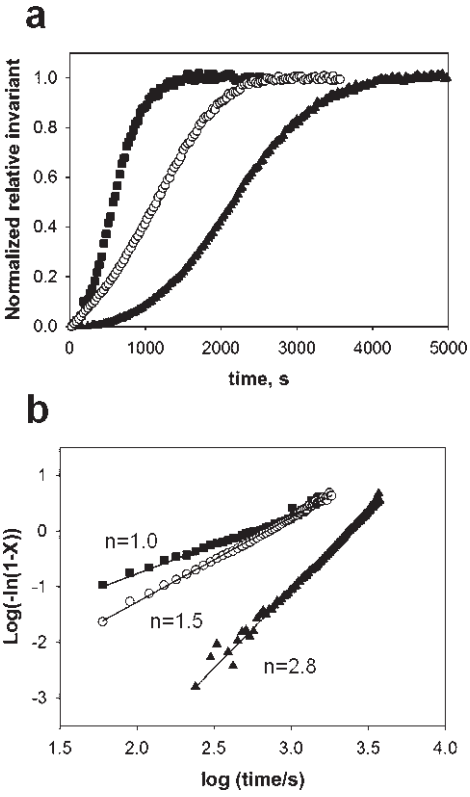

Figure 2. Effect of flow and partial relaxation on the progress of crystallization at 135 °C. (a) Normalized relative invariant as a function of crystallization time; (b) Avrami plot of the data shown in part a. Flow conditions: $\dot{\gamma} = 16\ s^{-1}$; $T_s = 170$ °C; $t_s = 5$ s. $T_R = 170$ °C. Quiescent crystallization (▲); $t_R = 0$: (■); $t_R = 30$ min (○).

coefficient have widely been reported in the literature on flow-induced crystallization.[16,58,60] In Figure 2b, the Avrami plots corresponding to the crystallization experiments of Figure 2a are shown. As expected, in quiescent conditions the Avrami exponent, n, is close to 3, indicating three-dimensional growth of predetermined nuclei; instead, for the unrelaxed sheared sample, $n \approx 1$, suggesting lower growth dimensionality or different growth mechanism. On increasing the holding time at the relaxation temperature a gradual increase of n toward the quiescent value has been observed in the whole set of experiments. To extract quantitative information on the kinetics of disappearance of flow-induced precursors from the above non avramian crystallization processes, we introduce the relative shear efficiency (RSE), a quantity which is related to the residual effect of shear on the crystallization rate constant defined by the dimensionless number:

$$\mathrm{RSE} = \frac{t_{0.5}(t_R) - t_{0.5}(q)}{t_{0.5}(t_{R=0}) - t_{0.5}(q)} \tag{4}$$

where $t_{0.5}(t_R)$, $t_{0.5}(t_{R=0})$ and $t_{0.5}(q)$ are the crystallization half-times measured in samples which have been relaxed at high temperature for a time t_R, for samples immediately quenched to T_c after shear and for the quiescent crystallization of unsheared samples, respectively. According to its definition, RSE values must lie between 0 (no effect of flow on crystallization kinetics, i.e., quiescent crystallization) and 1 (maximum shear efficiency, when no relaxation step is interposed between the shearing and the isothermal crystallization). RSE only reflects the relaxation phenomena leading to dissolution (disappearance) of flow-induced nuclei and does not provide information on their overall concentration, which is obviously dictated by the imposed flow

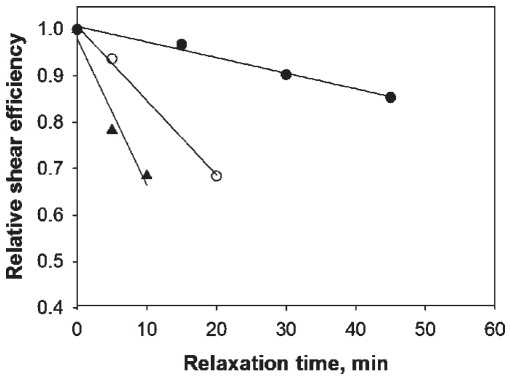

Figure 3. Relative shear efficiency as a function of time for different relaxation temperatures: $T_R = 170\,°C$ (●); $T_R = 180\,°C$ (○); $T_R = 190\,°C$ (▲). Flow conditions: $\dot{\gamma} = 32\ s^{-1}$; $T_s = 170\,°C$; $t_s = 5$ s. $T_c = 135\,°C$.

Table 1. Lifetime of Shear Induced-Precursors as a Function of Shear and Relaxation Conditions[a]

shear rate, s^{-1}	relaxation temperature, °C	rate constant k, min^{-1}	lifetime τ, s
32	170	0.0034	17500
32	180	0.016	3800
32	190	0.0315	1900
16	170	0.0114	5300
16	180	0.0432	1400

[a] All precursors were generated at 170 °C with a shear pulse of 5 s.

conditions: shear temperature, shear rate and shearing time. The results of relaxation experiments performed at 3 different temperatures on samples sheared under identical conditions (T_{shear}= 170 °C, $t_{shear} = 5$ s and shear rate $\dot{\gamma} = 32\ s^{-1}$) are shown in Figure 3. A linear decrease of RSE with increasing the duration of the relaxation step is observed for all the investigated temperatures. Clearly, this must be associated with the progressive dissolution of the unstable nucleation precursors injected into the molten polymer during the shearing step. It is also clear that the rate at which these flow-induced entities dissolve increases on increasing the temperature at which the system is held to relax. The lifetime of flow-induced nucleation precursors, that is obtained by extrapolating to RSE = 0 the straight lines of Figure 3, exhibits a marked temperature dependence, becoming shorter as the temperature is increased. This time, which characterizes the molecular processes behind precursor's dissolution, is remarkably longer than the rheological relaxation times. In fact at 170 °C, just above the melting temperature of i-PP crystals, several hours are needed to fully erase the effect of the imposed flow on crystallization kinetics and only about 30% of the shear effect is lost when the system is held to relax for 20 min at 180 °C. In this temperature range, the average rheological relaxation time of the used i-PP is of the order of one second.[53]

The rate constant, i.e., the value of the slope of RSE vs. time in the melt after shear, and the above-defined lifetime of flow-induced precursors are given in Table 1. They are well in line with those previously reported for the disappearance of transcrystallinity in fiber pulling experiments[49,50] and for the decay of shear-induced nuclei from rheo-optical measurements.[52]

According to our previous analysis, an Arrhenius type equation can be used to describe the temperature dependence of precursors' lifetime:[32,44,45,52]

$$\tau(T) = \tau_0 \exp\left(\frac{E_a}{RT}\right) \quad (5)$$

where R is the universal gas constant, T is the absolute temperature, and τ_0 is a material constant. From the data reported in Table 1, the value of the activation energy for precursors relaxation process is estimated to be around 210 ± 20 kJ/mol, apparently independent of the shear rate at which they have been generated. This value is consistent with those reported in the literature for the relaxation of different flow-induced structures in i-PP melts. Activation energies between 150 and 300 kJ/mol have been reported for shear-induced helical sequences of repeating units,[32] for threadlike precursors,[44,45] and for transcrystalline layers around pulled fibers.[49] It is important to remark that the activation energy of the relaxation process of flow-induced nucleation precursors is much greater than that of viscous flow, which is typically in the order of 40 kJ/mol. As previously suggested,[52] this discrepancy indicates that the rate-determining step in the relaxation mechanism is not the simple recovery of the unperturbed molecular conformation, but is rather related to detachment of chain segments from the lateral surfaces of quasi-crystalline flow-induced structures.

Experiments aimed at highlighting the role of shearing conditions on stability of shear induced nucleation precursors were also performed. Indeed, according to classical crystal nucleation theories,[61] the thermal stability of ordered clusters is related to their geometrical features, surface energies and degree of perfection which are likely dependent on the flow conditions in which they have been formed. This dependence has seldom been investigated. Li et al. observed a dual relaxation behavior of shear-induced helices in i-PP;[32] they assigned the longest decay time to dissolution of bundles of helices and the shortest to recoiling of isolated sequences of 3/1 helical conformations. Further studies suggest that the stability of helical conformations also depends on the number of repeating units in the sequence.[33] Size-dependent stability of shish structures was also found by Fu et al. who observed longer lifetime for the larger shishes produced at higher shear rates.[62] Recently, Balzano et al. reported that the aspect ratio of i-PP shishes and their stability in the melt increase with the shear stress.[63] By considering the lifetime of precursors generated under identical conditions but different shear rates given in Table 1, one notices that the stronger is the imposed shear flow, the slower is their disappearance. From these data it cannot unequivocally be established which is the relevant flow parameter responsible for the difference in precursors' stability. Indeed, varying the shear rate at constant shearing temperature and time implicitly changes the shear strain and, due to the pseudoplastic behavior, also the shear stress. Despite the above consideration, our data demonstrate the dependence of precursors' stability, and thus of their morphological and structural features, on flow conditions.

Effect of Flow and Relaxation on the Final Crystals Orientation. The 2-D SAXS patterns collected during the isothermal crystallization were used to calculate the Hermans orientation function, from which the lamellar orientation in the different series of experiments has been quantified. The evolution of the calculated orientation function is reported in Figure 4 for a system which has been relaxed after shear for increasing time periods. The common feature in the progress of crystallization of sheared systems is the progressive decrease of orientation of the whole population of lamellae.[13,65,66] This is consistent with rheo-optical observations which have shown that, provided the flow intensity is sufficiently high, oriented row-nucleated structures are the first to develop from a sheared melt.[7] Thus, the contribution of oriented crystals to the scattered intensity is maximum in the first stages of shear-induced crystallization, when lamellae mainly develop from oriented row-nuclei and the scattering by unoriented lamellae, originated from point-like nuclei, is negligible. The azimuthally independent scattering intensity, which arises from the branching of

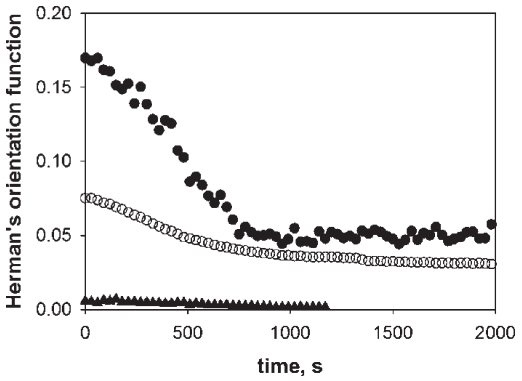

Figure 4. Evolution of the Hermans orientation function during isothermal crystallization at 135 °C, after a relaxation step at 180 °C: 0 min (●); 5 min (○); 20 min (▲). Flow conditions: $\dot{\gamma} = 32\ s^{-1}$; $T_s = 170$ °C; $t_s = 5$ s. The origin of the time axis corresponds to the time at which lamellae are first detected.

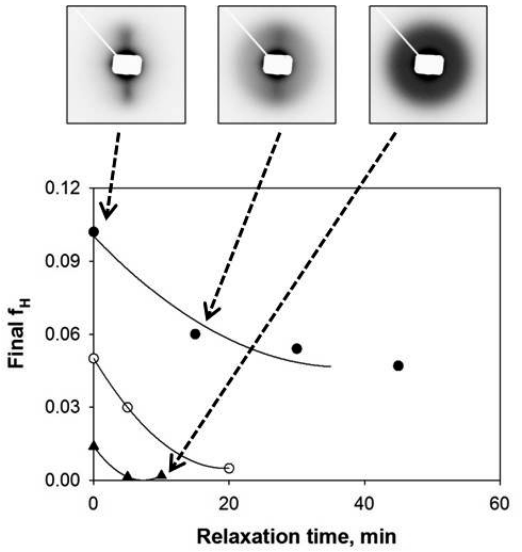

Figure 5. Effect of the annealing time on the overall orientation function at the end of crystallization. The samples were sheared at $T_s = 170$ °C for $t_s = 5$ s with $\dot{\gamma} = 32\ s^{-1}$. Relaxation temperatures: 170 °C (●); 180 °C(○); 190 °C (▲). Lines are drawn only to guide the eyes. Examples of representative 2D SAXS patterns are also shown.

row-nucleated lamellae and from the growing of isotropic spherulites, increases as the crystallization proceeds and eventually takes over the oriented contribution.

The progressive dissolution of flow-induced nucleation precursors slows down the crystallization kinetics and, in addition, has an impact on the resulting lamellar orientation. In fact, as shown in Figure 4, both initial and final values of the orientation factor decrease with increasing the holding time in the melt after shear. When no or very short relaxation is permitted, the lamellae which develop first are rather well oriented with their normal along the flow direction. On the other hand, after sufficiently long waiting time, unoriented morphology develops also in the early stages of crystallization due to disappearance of row-nuclei. The value of the Hermans orientation function at the end of the crystallization is plotted in Figure 5 as a function of the holding time in the melt at different temperatures, for a system which has been sheared under the very same conditions. These values are well in line with those usually observed in samples sheared in mild conditions such as those attainable with rotational plate−plate devices,[57] or in the intermediate/core regions of injection molded plaques.[64] The

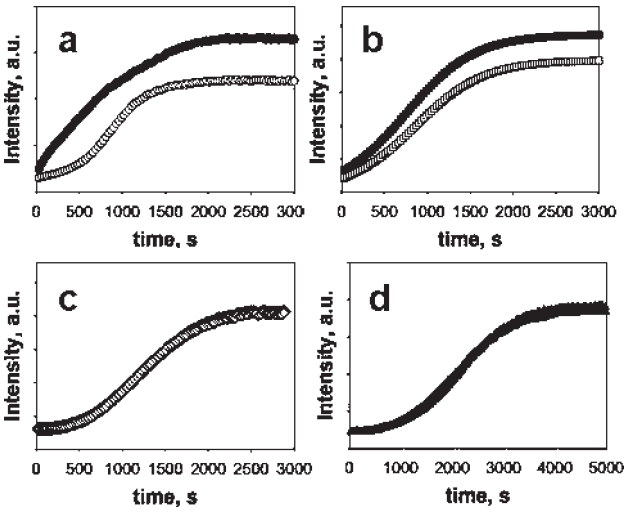

Figure 6. Intensity evolution for azimuthal sectors along the meridian (filled symbols) and the equatorial (open symbols) directions. The samples were sheared at 170 °C for 5s at a shear rate of 32 s^{-1} and crystallized isothermally at 135 °C. Relaxation temperature: 180 °C. Relaxation times: (a) 0 min; (b) 5 min; (c) 20 min; (d) quiescent crystallization.

orientation observed at zero holding time decreases with increasing holding temperature; this is due to the partial dissolution of oriented precursors, which takes place during the thermal transient necessary to reach the target temperature after shearing. Anyhow, it is well evident that the fraction of precursors which survives the heating process further decays with the holding time, leading to a progressive fading of the residual overall orientation. Straightforward evidence of these morphological effects is provided by the examples of 2D SAXD patterns reported in Figure 5. Samples held to relax at the highest temperature exhibit a faster decay of orientation, which eventually leads to a fully isotropic system in a relatively short time. An analogous behavior, albeit with a shift toward smaller orientation factors, was also found for samples sheared at the lower shear rate of 16 s^{-1}. Decrease of orientation function and slowing down of crystallization kinetics occur simultaneously; since they show analogous temperature dependence, it is reasonable to expect that they are governed by the same molecular mechanisms. However, this does not imply that the two phenomena happen in the same time scale. Indeed, by comparing the data of Figures 5 and 3, it can be appreciated that the time required to erase the effect of flow on lamellar orientation is much shorter than that needed to restore the quiescent crystallization kinetics. For example, while the orientation fully disappears by holding the sheared sample for 20 min at 180 °C, the crystallization kinetics is still considerably faster than that corresponding to quiescent conditions.

A further insight on the origin of the different time scales in which isotropic and quiescent crystallization kinetics are restored can be gained by separately analyzing the scattered intensity along the meridian, to which contribute oriented and unoriented lamellae, and along the equator, which results only from unoriented lamellae. In Figure 6 the intensities of the azimuthal sectors parallel and perpendicular to the flow direction, i.e. centered along the meridian and the equator, respectively, are plotted as a function of the crystallization time for samples with different extents of relaxation. For the unrelaxed sample, Figure 6a, the intensity evolution along the two directions is markedly different. As soon as the crystallization temperature is reached, the intensity along the meridian immediately increases and then gradually levels off; instead, the scattering in the equatorial sector follows a sigmoidal trend. This is consistent with an early onset of

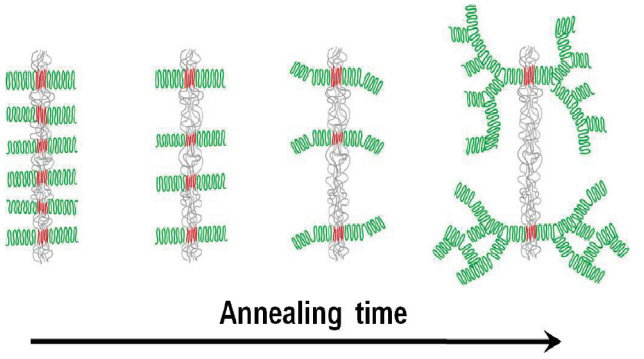

Figure 7. Schematic mechanism of precursor's relaxation and of its morphological implications.

the crystallization taking place from row-nuclei in comparison to that from point-like nucleation centers, as previously reported in the literature.[16,58,66] The final level of the two intensities is also different, obviously due to a non negligible overall lamellar orientation. On increasing the time of relaxation, the evolution of the two intensities becomes progressively similar, with a small prevalence of the meridional intensity (Figure 6b), and eventually they coincide (Figure 6c). At this stage of the relaxation process, even if no trace of anisotropic crystallization is detected, the kinetics of the phase transition is still much faster than that of the quiescent system (Figure 6d). Notwithstanding the different time scales involved in the disappearance of flow effects on morphology and on crystallization kinetics a common pathway can be argued. This is schematically illustrated in Figure 7.

Sufficiently strong shear acting on a molten polymer produces bundles of chain segments aligned in the flow direction, usually referred to as shishes, which provide nucleation sites for lamellar overgrowths.[15,34,35,48] Right after the cessation of shear, the linear density of these bundles, i.e. their number per unit length, is the highest; thus, as depicted on the left side of Figure 7, the closely spaced lamellae are bounded to develop in a perpendicular direction to form a cylindritic type of morphology.[49,52] The smaller and less ordered clusters disappear in the first stages of the relaxation step. Their dissolution causes an increase of the average distance between nucleation centers which should be reflected by an increase of the spacing between adjacent kebabs. Indeed, Zuo et al.[48] reported a long period increase in the crystallization from partially molten shish scaffolds in high molar mass polyethylene. This variation of the long period with the progress of the relaxation process was not revealed in our experiments probably due to the relatively low volume fraction of the row-nucleated structures. Further decrease of the concentration of shear-induced nuclei leads to a situation in which they are sufficiently far apart to enable 3D development of the morphology and, therefore, to absence of orientation (right side of Figure 7). This notwithstanding, the number of nuclei per unit volume, which now have a point-like character, can still be orders of magnitude larger than that found in quiescent conditions, this implying a much faster crystallization. Prolonged relaxation results in the disappearance of all the flow-induced precursors, thus restoring the quiescent crystallization rate.

This view is indirectly supported also by the progress of the isothermal crystallization at different stages of relaxation. The development of crystallinity is non avramian for the as sheared samples, becomes avramian with low growth dimensionality at intermediate relaxation stages and finally, when the crystalline morphology is isotropic, the classical 3D growth of predetermined nuclei is found.

Conclusions

The persistence of flow effects on i-PP crystallization, both on kinetics and overall orientation, has been investigated by acquiring 2D-SAXS patterns in isothermal crystallization experiments after the application of a controlled shear pulse on the molten polymer and a subsequent quiescent annealing at high temperatures. Prolonged annealing at high temperature eventually leads to unoriented morphology which develops with a kinetics approaching that of the unsheared polymer.

The annealing time necessary for the full erasure of flow memory at temperatures above the melting point of the crystals can be very long; several hours are required to restore equilibrium when annealing is performed at low superheating. In semiquantitative terms, the disappearance of the effect of shear on crystallization kinetics has been discussed by introducing the relative shear efficiency, RSE, a dimensionless parameter calculated from the half-crystallization times. As shown in Figure 3, the rate at which RSE decreases is strongly temperature-dependent, becoming faster with increasing the relaxation temperature. Both the time-scale of the process and its temperature dependence suggest that the mechanism governing disappearance of flow-induced precursors involves much more than the simple recovery of unperturbed coil conformation of molten polymer chains. It has also been observed that, at a given annealing temperature, the characteristic time for precursors' dissolution is larger for those which have been generated at higher shear rates. Again, this indicates that fading of flow memory is affected by the structural and morphological features of the precursors. On the other hand, the apparent activation energy of the relaxation process does not show significant differences in the range of imposed flow conditions, thus suggesting an analogous rate-determining step.

In parallel with the slowing down of crystallization kinetics, also the effect of shear on lamellar orientation vanishes with annealing time. Interestingly, the time required to restore isotropic crystallization is appreciably shorter than that needed to erase the memory of flow on the kinetics.

This can be explained by considering that the disappearance of row-nucleated precursors proceeds through a fragmentation mechanism which leaves progressively far apart point-like nuclei surviving inside the initial flow-induced threadlike structures. Therefore, the enhanced crystallization rate observed when the orientation is fully lost is ascribed to a concentration of point-like nuclei which still exceeds the quiescent nucleation density.

Acknowledgment. Authors are grateful to the European Community for financing the project II-05 047 EC at the beamline A2, DESY, Hamburg

References and Notes

(1) Keller, A.; Kolnaar, H. W. H. In *Materials Science and Technology. A Comprehensive Treatment*, Meijer, H. E. H., Vol. Ed.; Cahn, R. W., Haasen, P., Kramer, E. J., Series Eds.; VCH-Wiley: Weinheim, Germany, 1997; Vol. *18*, pp 189−268.
(2) Binsbergen, F. L. *Nature* **1966**, *211*, 516–517.
(3) Lagasse, R. R.; Maxwell, B. *Polym. Eng. Sci.* **1976**, *16*, 189–199.
(4) Fritzsche, A. K.; Price, F. P.; Ulrich, R. D. *Polym. Eng. Sci.* **1976**, *16*, 182–188.
(5) Lee, K. G.; Schultz, J. M. *Polymer* **1993**, *34*, 4455–4470.
(6) Samon, J. M.; Schultz, J. M.; Hsiao, B. S.; Seifert, S.; Stribeck, N.; Gurke, I.; Collins, G.; Saw, C. *Macromolecules* **1999**, *32*, 8121–8132.
(7) Pogodina, N. V.; Lavrenko, V. P.; Srinivas, S.; Winter, H. H. *Polymer* **2001**, *42*, 9031–9043.
(8) Acierno, S.; Palomba, B.; Winter, H. H.; Grizzuti, N. *Rheol. Acta* **2003**, *42*, 243–250.

(9) Elmoumni, A.; Winter, H. H.; Fruitwala, A. J. W. *Macromolecules* **2003**, *36*, 6453–6461.
(10) Coppola, S.; Balzano, L.; Gioffredi, E.; Maffettone, P. L.; Grizzuti, N. *Polymer* **2004**, *45*, 3249–3256.
(11) Vega, J. F.; Hristova, D. G.; Peters, G. W. M. *J. Therm. Anal. Calorim.* **2009**, *98*, 655–666.
(12) Housmans, J. W.; Steenbakkers, R. J. A.; Roozemond, P. R.; Peters, G. W. M.; Meijer, H. E. H. *Macromolecules* **2009**, *42*, 5728–5740.
(13) Somani, R. H.; Hsiao, B. S.; Nogales, A.; Srinivas, S.; Tsou, A. H.; Sics, I.; Balta-Calleja, F. J.; Ezquerra, T. A. *Macromolecules* **2000**, *33*, 9385–9394.
(14) Somani, R. H.; Hsiao, B. S.; Nogales, A.; Srinivas, S.; Tsou, A. H.; Balta-Calleja, F.; Ezquerra, T. A. *Macromolecules* **2001**, *34*, 5902–5909.
(15) Somani, R. H.; Yang, L.; Hsiao, B. S.; Agarwal, P. K.; Fruitwala, H. A.; Tsou, A. H. *Macromolecules* **2002**, *35*, 9096–9104.
(16) Balzano, L.; Rastogi, S.; Peters, G. W. M. *Macromolecules* **2009**, *42*, 2088–2092.
(17) Kumaraswamy, G.; Issaian, A. M.; Kornfield, J. A. *Macromolecules* **1999**, *32*, 7537–7547.
(18) Kumaraswamy, G.; Verma, R. K.; Issaian, A. M.; Wang, P.; Kornfield, J. A.; Yeh, F.; Hsiao, B. S.; Olley, R. H. *Polymer* **2000**, *41*, 8931–8940.
(19) Seki, M.; Thurman, D. W.; Oberhauser, J. P.; Kornfield, J. A. *Macromolecules* **2002**, *35*, 2583–2594.
(20) Baert, J.; Langouche, F.; Van Puyvelde, P. *Macromolecules* **2006**, *39*, 9215–9222.
(21) Fukushima, H.; Ogino, Y.; Matsuba, G.; Nishida, K.; Kanaya, T. *Polymer* **2005**, *46*, 1878–1885.
(22) Baert, J.; Van Puyvelde, P. *Polymer* **2006**, *47*, 5871–5879.
(23) Monasse, B. *J. Mater. Sci.* **1992**, *27*, 6047–6052.
(24) Varga, J.; Karger-Kocsic, J. *J. Mater. Sci., Lett.* **1994**, *13*, 1069–1071.
(25) Varga, J.; Karger-Kocsis, J. *J. Polym. Sci., Part B: Polym. Phys.* **1996**, *34*, 657–670.
(26) Koscher, E.; Fulchiron, R. *Polymer* **2002**, *43*, 6931–6942.
(27) Janeschitz Kriegl, H. *Crystallization Modalities in Polymer Melt Processing*; Springer Verlag: Vienna, 2009.
(28) Ziabicki, A.; Alfonso, G. C. *Macromol. Symp.* **2002**, *185*, 211–231.
(29) Wang, M.; Hu, W.; Ma, Y.; Ma, Y. Q. *Macromolecules* **2005**, *38*, 2806–2812.
(30) Chai, C. K.; Dixon, N. M.; Gerrard, D. L.; Reed, W. *Polymer* **1995**, *36*, 661–663.
(31) An, H.; Zhao, B.; Ma, Z.; Shao, C.; Wang, X.; Fang, Y.; Li, L.; Li, Z. *Macromolecules* **2007**, *40*, 4740–4743.
(32) An, H.; Li, X.; Geng, Y.; Wang, Y.; Wang, X.; Li, L.; Li, Z.; Yang, C. *J. Phys. Chem. B* **2008**, *112*, 12256–12262.
(33) Geng, Y.; Wang, G.; Cong, Y.; Bai, L.; Li, L.; Yang, C. *Macromolecules* **2009**, *42*, 4751–4757.
(34) Somani, R. H.; Yang, L.; Hsiao, B. S. *Physica A* **2002**, *304*, 145–157.
(35) Somani, R. H.; Sics, I.; Hsiao, B. S. *J. Polym. Sci., Part B: Polym. Phys.* **2006**, *44*, 3553–3570.
(36) Balzano, L.; Kukalyekar, N.; Rastogi, S.; Peters, G. W. M.; Chadwick, J. C. *Phys. Rev. Lett.* **2008**, *100*, 048302–048304.
(37) Fernàndez-Ballester, L. Ph.D. Thesis, California Institute of Technology, 2007.
(38) Kanaya, T.; Takayama, Y.; Ogino, Y.; Matsuba, G.; Nishida, K. In *Progress of Understanding of Polymer Crystallization*; Lecture Notes in Physics 714; Reiter, G., Strobl, G. R., Eds.; Springer: Berlin and Heidelberg, Germany, 2007; pp 87−96.
(39) Hayashi, Y.; Matsuba, G.; Zhao, Y.; Nishida, K.; Kanaya, T. *Polymer* **2009**, *50*, 2095–2103.
(40) Janeschitz-Kriegl, H.; Wimberger-Friedl, R.; Krobath, G.; Liedauer, S. *Kautsch. Gummi Kunstst.* **1987**, *40*, 301–307.
(41) Eder, G.; Janeschitz-Kriegl, H.; Krobath, G. *Prog. Colloid Polym. Sci.* **1989**, *80*, 1–7.
(42) Eder, G.; Janeschitz-Kriegl, H.; Liedauer, S. *Prog. Polym. Sci.* **1990**, *15*, 629–714.
(43) Braun, J.; Wippel, H.; Eder, G.; Janeschitz-Kriegl, H. *Polym. Eng. Sci.* **2003**, *43*, 188–203.
(44) Janeschitz-Kriegl, H.; Eder, G. *J. Macromol. Sci., Part B Phys.* **2007**, *46*, 591–601.
(45) Isayev, T.; Chan, W.; Shimojo, K.; Cmerek, M. *J. Appl. Polym. Sci.* **1995**, *55*, 807–819.
(46) Sajkiewicz, P.; Wasiak, A.; Kukla, D.; Boguszewsky, M. *J. Mater. Sci., Lett.* **2000**, *19*, 847–849.
(47) Chai, C. K.; Auzoux, Q.; Randrianatoandro, H.; Navard, P.; Haudin, J. M. *Polymer* **2003**, *44*, 773–782.
(48) Zuo, F.; Keum, J. K.; Yang, L.; Somani, R. H.; Hsiao, B. S. *Macromolecules* **2006**, *39*, 2209–2219.
(49) Alfonso, G. C.; Scardigli, P. *Macromol. Chem. Phys., Macromol. Symp.* **1997**, *118*, 323–328.
(50) Azzurri, F.; Alfonso, G. C. *Macromolecules* **2005**, *38*, 1723–1728.
(51) Garcıa Gutierrez, M. C.; Alfonso, G. C.; Riekel, C.; Azzurri, F. *Macromolecules* **2004**, *37*, 478–485.
(52) Azzurri, F.; Alfonso, G. C. *Macromolecules* **2008**, *41*, 1377–1383.
(53) Titomanlio, G.; Lamberti, G. *Rheol. Acta* **2004**, *43*, 146–158.
(54) http://www.esrf.eu/computing/scientific/FIT2D/
(55) Bark, M.; Zachmann, H. G.; Alamo, R.; Mandelkern, L. *Makromol. Chem.* **1992**, *193*, 2363–2377.
(56) Keates, P.; Mitchell, G. R.; Peuvrel-Disdier, E.; Navard, P. *Polymer* **1993**, *34*, 1316–1319.
(57) Mykhaylyk, O. O.; Chambon, P.; Impradice, C.; Fairclough, J. P. A.; Terril, N. J.; Ryan, A. J. *Macromolecules* **2010**, *43*, 2389–2405.
(58) Keum, J. K.; Zuo, F.; Hsiao, B. S. *Macromolecules* **2008**, *41*, 4766–4776.
(59) Lamberty, G.; Titomanlio, G. *Polym. Bull.* **2004**, *52*, 443–449.
(60) Heeley, E. L.; Fernyhough, C. M.; Graham, R. S.; Olmsted, P. D.; Inkson, N. J.; Embery, J.; Groves, D. J.; McLeish, T.C. B.; Morgovan, A. C.; Meneau, F.; Bras, W.; Ryan, A. J. *Macromolecules* **2006**, *39*, 5058–5071.
(61) Clark, E. K.; Hoffman, J. D. *Int. J. Thermophys.* **1990**, *11*, 225–237.
(62) Na, B.; Wang, Y.; Zhang, Q.; Fu, Q. *Polymer* **2004**, *45*, 6245–6260.
(63) Balzano, L.; Cavallo, D.; Van Erp, T. B.; Housmans, J. W.; Fernandez-Ballester, L.; Peters, G. W. M. *J. Phys.: Condens. Matter* **2010**, in press.
(64) Zhong, G. J.; Li, Z. M.; Li, L. B.; Mendes, E. *Polymer* **2007**, *48*, 1729–1740.
(65) Somani, R. H.; Yang, L.; Hsiao, B. S. *Polymer* **2006**, *47*, 5657–5668.
(66) Matsuba, G.; Sakamoto, S.; Ogino, Y.; Nishida, K.; Kanaya, T. *Macromolecules* **2007**, *40*, 7270–7275.